Proceedings of the 2011 IEEE
International Conference on Mechatronics and Automation
August 7 - 10, Beijing, China

Advanced Inversion Control for a Hypersonic Vehicle Based on PSO and Arranged Transient Process

Zhiqiang Pu, Xiangmin Tan, Jianqiang Yi, Guoliang Fan

Institute of Automation, Chinese Academy of Sciences, Beijing,100190, China

E-mail: zhiqiang.pu@ia.ac.cn

***Abstract* - A high-order curve-fitted model which is suitable for a large flight envelope is adopted for the aerodynamic coefficients of the Generic Hypersonic Vehicle (GHV). As a supplement, the expressions of the thrust coefficients for the whole hypersonic flight range are presented in this paper. Based on this model, a general Nonlinear Dynamic Inversion (NDI) controller is designed with the feedback linearization theory for the velocity and altitude tracking purpose. However, the robustness of this general NDI controller needs to be improved, particularly when a large step command is given. For these reasons, an advanced inversion controller is designed, where both the Particle Swarm Optimization (PSO) algorithm and Arranged Transient Process (ATP) technique are applied. The PSO is used to optimize the feedback coefficients of the inversion controller, while the ATP technique is employed to guarantee that the system has better dynamic performance and control quality. Simulation results demonstrate that the advanced inversion controller has better tracking performance and robustness in a large envelope of flight condition.**

***Index Terms* - Hypersonic Vehicle, Dynamic Inversion, Particle Swarm Optimization, Arranged Transient Process**

I. INTRODUCTION

Air-breathing hypersonic vehicles may eventually allow dramatic reductions in flight time for both commercial and military applications. Direct access to earth orbit without the use of separate boosting stages may also become possible as scramjet-powered aircraft enters service [1]. However, hypersonic air vehicles are sensitive to changes in flight condition as well as physical and aerodynamic parameters due to their design and flight conditions of high altitude and Mach number [2][3]. Strong couplings between propulsive and aerodynamic forces result from the underslung location of the scramjet engine [3]. Most dynamic models of interest are shown to be unstable and of non-minimum phase with respect to the variables to be controlled [4]. In addition, significant uncertainties affect the model as a result of the variability of the vehicle characteristics with the flight conditions, fuel consumption, and thermal effects on the structure. Therefore, the design of control law is really a challenging work.

In the literature, there have been many papers that discuss the model and control design for the Generic Hypersonic Vehicle (GHV). As a linearization tool, dynamic inversion control based on differential geometry theory has been widely used in hypersonic vehicle controllers, such as in [1], [2], [5], and [6]. To overcome the parameter uncertainty, an adaptive sliding mode controller on the basis of feedback linearization was developed in [2] and [7]. However, only one fixed cruising flight condition was considered in the coefficient model, which means, the controller might fail at another flight point. Such problem also lies in many other researches. As a technical memorandum, [8] offered detailed description about the winged-cone configuration GHV developed at NASA Langley Research Center. Unfortunately, there were only rough curves, rather than look-up tables or precise data. Keshmiri et al. [9] presented analytical expressions of the aerodynamic coefficients reposing on data in [7], but the expressions of the thrust coefficients were not presented.

In this paper, we present the analytical expressions of the thrust coefficients on the basis of the NASA memorandum. These curve-fitted expressions, together with other high-order aerodynamic coefficients in [9], are applicable in the whole hypersonic flight range.

Based on this high-order coefficient model, a general Nonlinear Dynamic Inversion (NDI) controller is designed for the velocity and altitude tracking purpose. Although this system can overcome a certain degree of parametric uncertainty with appropriate closed-loop poles, it is hard to select the optimal parameters without sufficient experiences. In addition, the NDI controller may be degraded in the presence of a higher level of parametric uncertainty or a larger step command.

The main contribution of this work is therefore to design an advanced inversion controller on the basis of the high-order coefficient model. Two strategies are incorporated into this advanced controller to improve the general NDI controller. The PSO algorithm [10] is applied to search the optimal feedback coefficients for the inversion controller. On the other hand, to arrange a transient process for the system is an effective method to improve the robustness, adaptability, and stability of the closed-loop system [11]. By arranging an appropriate transient process, we can resolve the conflict between rapidity and overshoot. Moreover, the applicable parameter space becomes larger and the tuning work becomes easier.

Ⅱ. HYPERSONIC VEHICLE MODEL

A model for the longitudinal dynamics of a generic hypersonic vehicle developed at NASA Langley Research Center is investigated in this paper. The aerodynamic characteristics of the winged-cone configuration hypersonic vehicle described in [8] make the modelling very challenging. The longitudinal dynamics can be described by a set of differential equations as [2][12]:

$$\dot{V} = \frac{T\cos\alpha - D}{m} - \frac{\mu \sin\gamma}{r^2} \tag{1}$$

$$\dot{\gamma} = \frac{L + T\sin\alpha}{mV} - \frac{(\mu - V^2 r)\cos\gamma}{Vr^2} \tag{2}$$

$$\dot{h} = V\sin\gamma \tag{3}$$

$$\dot{\alpha} = q - \dot{\gamma} \tag{4}$$

$$\dot{q} = \frac{M_{yy}}{I_{yy}} \tag{5}$$

where the states V, γ, h, α, and q respectively denote the velocity, flight-path angle, altitude, angle of attack, and pitch rate. Expressions of the lift L, drag D, engine thrust T, and pitch moment M_{yy} will be given later.

The engine dynamics can be written as a second-order system:

$$\ddot{\phi} = -2\xi\omega\dot{\phi} - \omega^2\phi + \omega^2\phi_c \tag{6}$$

Parametric uncertainty is also modelled as an additive variance Δ to the nominal values. The additive uncertainties are taken as follows:

$$\begin{cases} m = m_0(1+\Delta m) \\ I_{yy} = I_0(1+\Delta I) \\ S_{ref} = S_0(1+\Delta S) \\ \bar{c} = \bar{c}_0(1+\Delta\bar{c}) \\ \rho = \rho_0(1+\Delta\rho) \end{cases} \tag{7}$$

As known, the aerodynamic coefficients are sensitive to changes in flight condition. In many researches, only one flight condition is considered, such as in [2] and [6]. That means the model is only suitable for one operating condition. Hence, if the flight condition, for example the velocity, takes a slightly large change, the model does not fit the practical situation and the controller may fail. Shaughnessy et al. [8] provided comprehensive CFD study results in the form of curve figures covering all of the subsonic, supersonic, and hypersonic flight conditions. As a trusted data source, this could be a good model reference.

The lift force, drag force, thrust, and pitch moment in [7] are computed as follows:

$$L = \bar{q}S_{ref}C_L \tag{8}$$

$$D = \bar{q}S_{ref}C_D \tag{9}$$

$$T = \bar{q}C_T \tag{10}$$

$$M_{yy} = \bar{q}cS_{ref}C_m \tag{11}$$

where

$$C_L = C_{La} + C_{L,de} + C_{L,da} \tag{12}$$

$$C_D = C_{Da} + C_{D,de} + C_{D,da} + C_{D,dr} \tag{13}$$

$$C_m = C_{ma} + C_{m,de} + C_{m,da} + C_{m,dr} + C_{m_q}(\frac{qc}{2V}) \tag{14}$$

In (12)-(14), the total aerodynamic coefficients all comprise several terms. Take (12) for example: the coefficients C_{La}, $C_{L,de}$, $C_{L,da}$, and C_L respectively denote the basic vehicle lift increment coefficient, the increment coefficient for the right elevator, the increment coefficient for the left elevator, and the total lift coefficient. Each coefficient is a function of several variables. Keshmiri et al. [9] presented their analytical expressions as up to fifth order polynomials based on the minimum values of Sum of Squares due to Error (SSE). Here we will not list these expressions due to the page limitation.

Unfortunately, [9] did not present the engine thrust expression. For this specific reason, we develop a MATLAB program to compute the thrust coefficients for the hypersonic flight range in this paper. The LSM optimization method is employed and the original data are still from the NASA report. Assume the thrust coefficient has the following form

$$C_T = \begin{cases} a_1\phi, & \phi \le 1 \\ a_2\phi + (a_1 - a_2), & \phi > 1 \end{cases} \tag{15}$$

where ϕ denotes the fuel equivalence ratio. Using the LSM program, we obtain the expressions of a_1 and a_2 as

$$a_1 = -0.0591M_a^3 + 3.2829M_a^2 - 62.6281M_a + 475.1407 \tag{16}$$

$$a_2 = -0.0111M_a^3 + 0.5982M_a^2 - 9.8995M_a + 66.5629 \tag{17}$$

Obviously, the thrust is closely related to the Mach number. An important fact is that, the effect of angle of attack is neglected in the above thrust coefficient expression. It makes sense because for speeds above $M_a = 4.00$ up to $M_a = 24.00$ a rocket engine cycle rather than the ramjet engine is used [9].

Comparison study shows that our result matches well to both the NASA CFD data and other one-point cases such as in [2]. Now we have a model with expressions covering a large flight envelope. This is the basis to do further research.

Ⅲ. FEEDBACK LINEARIZATION

From (1) to (5) we can find that the longitudinal model of the hypersonic vehicle is highly nonlinear and contains multiple inner couplings. As a generic tool, feedback linearization is used in this paper to get a linear model. Here we take the velocity and altitude as the output dynamics. Following the approach in [6], we differentiate the velocity three times and the altitude four times to make the control variables appear in the resulting equations explicitly. Then we get the following standard linearization equation:

$$\begin{bmatrix} \dddot{V} \\ h^{(4)} \end{bmatrix} = \begin{bmatrix} \dddot{V}_0 \\ h_0^{(4)} \end{bmatrix} + \begin{bmatrix} b_{11} & b_{12} \\ b_{21} & b_{22} \end{bmatrix} \begin{bmatrix} \delta_e \\ \phi_c \end{bmatrix} = F_0 + BU \tag{18}$$

where δ_e is the elevator deflection and ϕ_c denotes the command of fuel equivalence ratio. The expressions of $\dddot{V}_0$, $h_0^{(4)}$ and b_{11}, b_{12}, b_{21}, b_{22} can be found in [6]. Assuming B is nonsingular, we select the feedback control law as

$$U = B^{-1}(v - F_0) \tag{19}$$

where $v = \begin{bmatrix} v_1 & v_2 \end{bmatrix}^T$ is the new control input vector. Then (18) reduces to the following linear input-output map:

$$\begin{bmatrix} \dddot{V} & h^{(4)} \end{bmatrix}^T = \begin{bmatrix} v_1 & v_2 \end{bmatrix}^T = v \tag{20}$$

Furthermore, the map obtained in (20) can be written as a new integrator-decoupled system by defining a set of nonlinear transformations as

$$\begin{cases} X_1 = e_V \\ X_2 = \dot{e}_V \\ X_3 = \ddot{e}_V \end{cases} \tag{21}$$

$$\begin{cases} Y_1 = e_h \\ Y_2 = \dot{e}_h \\ Y_3 = \ddot{e}_h \\ Y_4 = \dddot{e}_h \end{cases} \tag{22}$$

where $e_V = V - V_d$ and $e_h = h - h_d$. V_d and h_d respectively denote the reference velocity and altitude signals. Define $X = [e_V \quad \dot{e}_V \quad \ddot{e}_V]^T$ and $Y = [e_h \quad \dot{e}_h \quad \ddot{e}_h \quad \dddot{e}_h]^T$. We get the following Brunovsky canonical form by differentiating (21):

$$\dot{X} = A_1 X + B_1 W_1 \tag{23}$$

where

$$A_1 = \begin{bmatrix} 0 & 1 & 0 \\ 0 & 0 & 1 \\ 0 & 0 & 0 \end{bmatrix}, \quad B_1 = \begin{bmatrix} 0 \\ 0 \\ 1 \end{bmatrix}, \quad W_1 = v_1 - \ddot{V}_d$$

By differentiating (22) we get

$$\dot{Y} = A_2 Y + B_2 W_2 \tag{24}$$

where

$$A_2 = \begin{bmatrix} 0 & 1 & 0 & 0 \\ 0 & 0 & 1 & 0 \\ 0 & 0 & 0 & 1 \\ 0 & 0 & 0 & 0 \end{bmatrix}, \quad B_2 = \begin{bmatrix} 0 \\ 0 \\ 0 \\ 1 \end{bmatrix}, \quad W_2 = v_2 - h_d^{(4)}$$

Equation (23) and (24) represent two linear systems. In this paper, we design W_1 and W_2 by configuring the poles of the linear systems. Reposing upon the state feedback theory, the control law of the linear systems can be written as

$$\begin{cases} W_1 = v_1 - \ddot{V}_d = KV_0 e_V + KV_1 \dot{e}_V + KV_2 \ddot{e}_V \\ W_2 = v_2 - h_d^{(4)} = KH_0 e_h + KH_1 \dot{e}_h + KH_2 \ddot{e}_h + KH_3 \dddot{e}_h \end{cases} \tag{25}$$

where KV_0, KV_1, KV_2 and KH_0, KH_1, KH_2, KH_3 are the state feedback coefficients. Then v is obtained as

$$v = \begin{bmatrix} v_1 \\ v_2 \end{bmatrix} = \begin{bmatrix} KV_0 e_V + KV_1 \dot{e}_V + KV_2 \ddot{e}_V + \ddot{V}_d \\ KH_0 e_h + KH_1 \dot{e}_h + KH_2 \ddot{e}_h + KH_3 \dddot{e}_h + h_d^{(4)} \end{bmatrix} \tag{26}$$

Taking v back into (19), we get the control inputs for the original model.

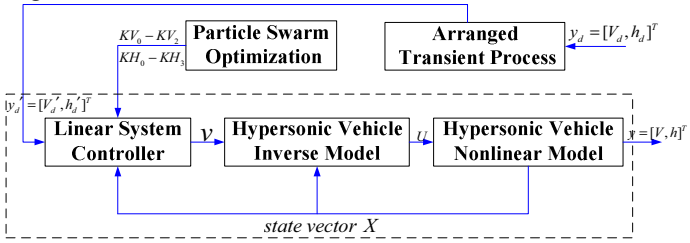

Fig. 1 System structure

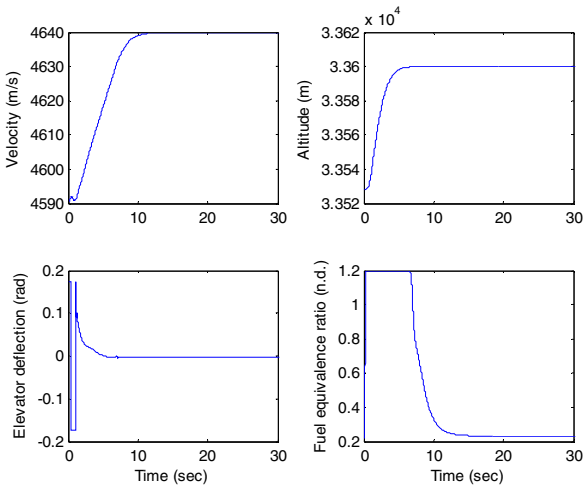

Fig. 2 General NDI controller with parameter uncertainty

Fig. 1 depicts the structure of the complete closed-loop system. The block in the dashed rectangle indicates the general NDI control system discussed in this section. The PSO is used to optimize the full state feedback coefficients, and the ATP technique can guarantee the system has better dynamic performance and control quality, both of which will be discussed in the next section.

In this general NDI system, the nominal flight of the vehicle is at a trimmed cruise condition [2] ($V = 4590m/s$, $h = 33528m$, $\gamma = 0rad$, and $q = 0rad/s$). The reference velocity and altitude are set as $V_d = 4640m/s$ and $h_d = 33600m$. Two constraints are respectively placed on the elevator deflection ($|\delta_e| \le 10\deg$) and the fuel equivalence ratio ($0 \le \phi_c \le 1.2$). The parametric uncertainty is also considered and the worst case occurs when Δm and ΔI take their maximum negative values, while $\Delta\rho$, ΔS, and $\Delta\bar{c}$ take their maximum positive values [2]. The feedback coefficients KV_0, KV_1, KV_2 and KH_0, KH_1, KH_2, KH_3 are respectively set at 6, 11, 6 and 24,50,35,10. Simulation results in Fig. 2 show that the closed-loop system can endure up to 10% parameter uncertainty due to a certain degree of stability margin with an appropriate group of poles. It must be noted that there lies an actuator saturation problem, which can be overcome with anti-windup control methods [13].

Although the general NDI controller can stabilize the system with some degree of parameter uncertainty, the stability margin depends on the feedback coefficients, which determine the positions of closed-loop poles. However, it is difficult to find the best poles without enough experiences. In addition, the dynamic performance and control quality need to be improved. Particularly, when a slightly large step command is given, the general NDI controller may fail in stabilizing the system. For these reasons, an advanced dynamic inversion controller is designed in the next section, where both the PSO algorithm [10] and ATP technique [11] are adopted.

IV. Advanced Inversion Control

A. Particle Swarm Optimization

In the general NDI controller, there are seven feedback coefficients KV_0, KV_1, KV_2 and KH_0, KH_1, KH_2, KH_3 which determine the poles and affect the system performance directly. In this section, we will set the initial values for these coefficients based on a rough evaluation of the poles, and the optimal coefficients will be found with PSO algorithm.

Because of the complication of the control model and the lack of flight test data, some adaptive approaches such as neural network control are time consuming and not practical. The PSO algorithm [10], which was introduced by Eberhart and Kennedy in 1995, has a better global convergence and a faster search speed when the training data are insufficient. The PSO is believed to be effective in multidimensional, linear, and nonlinear problems.

The particle swarm optimization is executed in the following process:

1) Initialization: Set the maximum generation $N_i = 100$, the population size $N_p = 50$, and the dimension of solution space $N_d = 7$. The initial particle positions are based on a rough evaluation of the poles. The solution space is limited between 0 and 60, and the maximum flight velocity $v_{\max}$ is 15% of the solution space. We should also set the individual learning factor c_1, social learning factor c_2, and the upper and lower bounds of the inertia weight factor $w_{\max}$ and $w_{\min}$. Later we will discuss the effects of these parameters.

2) Calculating the Fitness: It is quite important to choose the fitness function properly. There are several performance indexes for different types of control specification, such as Integral of Squared Error (ISE), Integral of Absolute Error (IAE), and Integral of Time-weighted Absolute Error (ITAE). Here we define an improved ITAE performance index as:

$$J = \int_0^\infty t(|\bar{e}_V| + |\bar{e}_h| + w_q|\bar{e}_q| + w_a|\bar{e}_a| + w_\gamma|\bar{e}_\gamma|)dt \qquad (27)$$

where $\bar{e}_V$, $\bar{e}_h$, $\bar{e}_q$, $\bar{e}_a$, and $\bar{e}_\gamma$ are the normalized errors of the velocity, altitude, pitch rate, angle of attack, and flight-path angle. Three tips of improvement should be emphasized. First, we take not only the output errors but also the state errors into consideration, which can guarantee the state variables, namely the pitch rate, angle of attack, and flight-path angle, have good transient processes. Second, we take the normalized errors rather than the realistic errors into consideration, because these five errors are quite different in magnitude, and normalization can make them equally important. Third, the weights w_q, w_a, and w_γ can flexibly adjust the contribution of the state errors to the performance index.

3) Finding out the Best Solution: Find and update the local best solution *pbest* and global best solution *gbest* according to the fitness value.

4) Updating the Velocity and Position: We update the velocity and position with the following equations:

$$v_i(k+1) = wv_i(k) + c_1r_1(pbest_i(k) - x_i(k)) + c_2r_2(gbest_i(k) - x_i(k)) \qquad (28)$$

$$x_i(k+1) = x_i(k) + v_i(k+1) \qquad (29)$$

$$w = w_{\max} - \frac{w_{\max} - w_{\min}}{N_i}k \qquad (30)$$

where $v_i(k)$ and $x_i(k)$ respectively denote the velocity and position of the particle i at generation k. The first term of (28), $wv_i(k)$, represents the velocity influence of the current generation to the next generation. Here the weight varies as (30) shows. Hence, at the beginning the velocity is large, which is beneficial to search solutions in a larger space; in the end the velocity becomes smaller to guarantee the convergence of the iteration. The second term of (28) indicates the individual learning behaviour, while the third term presents the social learning behaviour.

5) Termination condition: Go back to calculate the fitness again until the termination condition is satisfied, that is, the iteration goes to the end or the optimal parameters are found.

In this study, the initial feedback coefficients are chosen as those in the general NDI controller. The final parameters found by PSO are 16.8438, 22.0939, 12.0572 and 25.4964, 45.6975, 31.3464, 11.6699. The fitness function and results of comparison simulation are depicted in Figs. 3 and 4. Results indicate that the PSO-controller can not only guarantee both the output dynamics and state variables have better dynamic processes, but also give the system a wider stability margin.

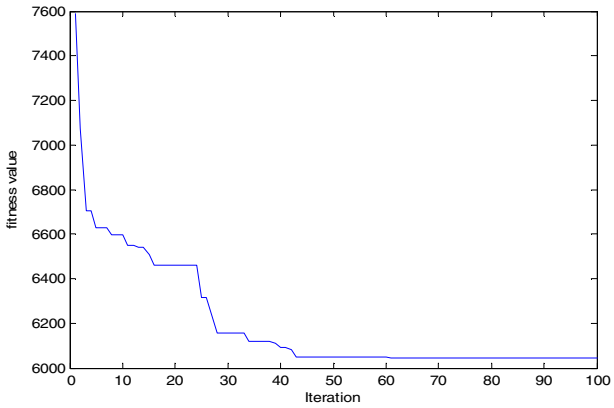

Fig. 3 Curve of the fitness function

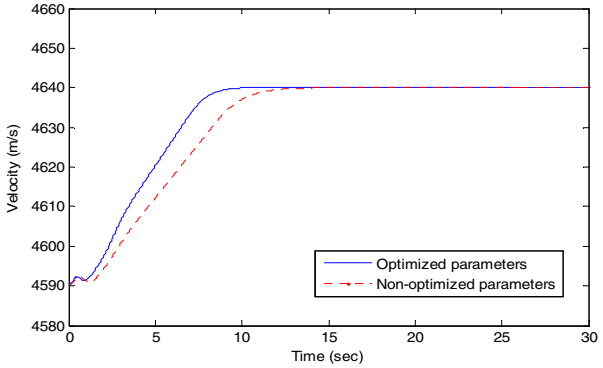

Fig. 4 Response to a step-velocity command

In this study we find the PSO iteration is easy to be trapped into local convergence, so as that the algorithm stops searching for new solutions. To avoid this prematurity case, we can increase the maximum velocity $v_{\max}$, decrease the social learning factor c_2, and select the appropriate upper and lower bounds of the inertia weight factor $w_{\max}$ and $w_{\min}$.

B. The Arranged Transient Process

In the foregoing controller, we use the direct errors between the outputs and reference inputs to design the control law. This may cause overshoot because the error at the beginning stage is often large. If we decrease the control parameters to eliminate this overshoot, the transient process may become longer. Therefore, it seems that there is always a conflict between rapidity and overshoot. Another problem is that, although we have got the optimal control parameters using PSO algorithm, the performance still may get worse if a larger step command is given to the system. That means the applicable parameter space is limited in a small range. In other words, the robustness needs to be improved.

In this paper, we take the Arranged Transient Process approach [11] to solve the aforementioned problems. The core idea is that, if we can arrange an appropriate transient process according to the step command and control ability, and let the outputs track the arranged transient process rather than the direct step command, then we can improve the robustness, adaptability, and stability of the closed-loop system.

To be brief, our purpose is to design a transient process and let the output dynamics, namely the velocity and altitude, track this arranged transient process. As known, the step response is closely related to the system order, so it is vital to consider the system order when a transient process is arranged. Here we take the following function as the desired transient process [11]:

$$r(t)=\begin{cases} 2\dfrac{r_0}{T^2}t^2, & t\le\dfrac{T}{2} \\ r_0(-2\dfrac{t^2}{T^2}+4\dfrac{t}{T}-1), & \dfrac{T}{2}<t\le T \\ r_0, & t>T \end{cases} \tag{31}$$

where T is the transient time, r_0 is the step value, and $r(t)$ is the arranged transient process. In addition, the derivatives of the output dynamics should also track the corresponding derivatives of the transient process in (31). Here we will not list the derivatives of $r(t)$ due to the page limitation.

Now consider responses to a large step command. In this study, we give a 150m/s step-velocity command and a 172m step-altitude command, so the reference velocity is 4740m/s and the reference altitude is 33700m. We carefully choose the transient time as $T_V=8s$ and $T_h=11s$. We compare the ATP-controller (the dynamic inversion controller based on PSO algorithm and ATP approach) with the PSO-controller (the dynamic inversion controller only based on PSO algorithm). Results are shown in Figs. 5 and 6.

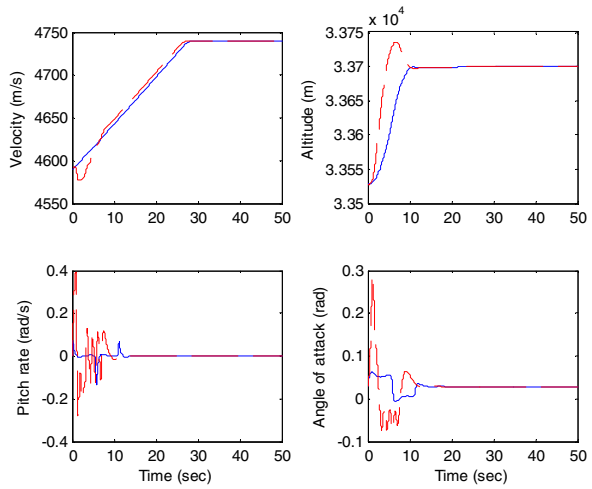

Fig. 5 Output and state variables of the comparison research. Solid curves are responses in the ATP-controller, while dashed curves are responses in the PSO-controller.

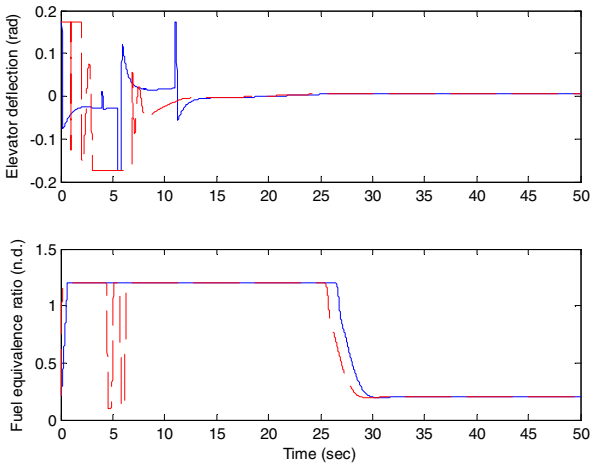

Fig. 6 Control variables of the comparison research. Solid curves are responses in the ATP-controller, while dashed curves are in the PSO-controller.

Fig. 5 displays the output and state variables. It is obvious that the ATP-controller makes the transient process smoother, that is, no overshoot, undershoot, or sharp chattering, particularly in the pitch rate and angle of attack responses. It is worth noting that the transient time is not shortened as desired, which is due to the actuator saturation. Fig. 6 shows the control variables. The control inputs vary fast in PSO-controller, particularly in the fuel equivalence ratio. This is not desired in engineering practice as the actuators cannot follow such a fast pace, thus the desired control target cannot be achieved. Results demonstrate that, by arranging appropriate transient processes, we can improve the dynamic performance, control quality, and parameter adaptability of the system.

We keep on increasing the reference commands to 4900m/s and 37000m, that is, a 310m/s step-velocity command and a 3472m step-altitude command. Simulation result is shown in Fig. 7. In this case, the ATP-controller can still work well, while the PSO-controller loses its control ability.

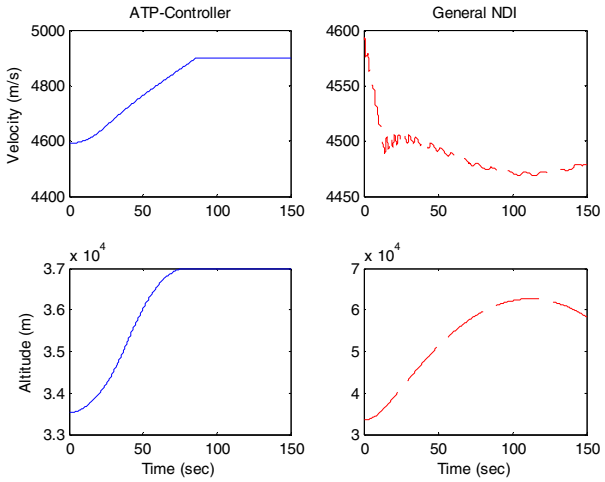

Fig. 7 Response to a 310m/s step-velocity command and a 3472m step-altitude command.

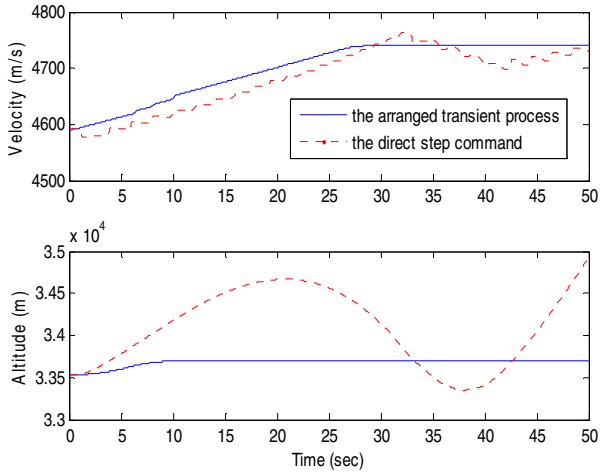

Fig. 8 Response with the increased control parameters.

Now consider changing the control parameters rather than the step commands. In the PSO-controller, the optimized parameters KH_0, KH_1, KH_2, and KH_3 are 25.4964, 45.6975, 31.3464, and 11.6699, and we respectively increase them to 120,154,71, and 14, which is a large change in control parameters. Simulation result is shown in Fig. 8. In this case, The ATP-controller can still stabilize the system, while the PSO-controller is degraded and the general NDI controller becomes even worse. This study indicates the ATP system has a larger parameter space to ensure the system stability, thus tunning the system can be much easier.

V. Conclusions

In this paper we have designed an advanced dynamic inversion controller for a kind of generic hypersonic vehicle based on the particle swarm optimization and the arranged transient process. First we have adopted and improved a high-order curve-fitted aerodynamic coefficients model on the basis of the NASA CFD database, which is applicable for a large flight envelope rather than one fixed flight point. Then we use the PSO algorithm to optimize the feedback coefficients of the general NDI controller, which can provide wider stability margin and better dynamic performance. At last, on the basis of the PSO-controller, we carefully arrange the transient process for the output dynamics. This ATP-controller not only makes the output, state, and control variables much smoother, but also enlarges the space of applicable control parameters.

Acknowledgment

This work was supported by the grants of the Knowledge Innovation Program of Chinese Academy of Sciences (No. ZKYGC09A02) and National Natural Science Foundation of China (No. 60904006).

References

[1] Jason T.Parker, Andrea Serrani, Stephen Yurkovich, Michael A.Bolender and David B.Doman, "Approximate feedback linearization of an air-breathing hypersonic vehicle," *AIAA Guidance, Navigation and Control Conference and Exhibit*, AIAA 2006-6556, 21-24 August 2006.

[2] Haojian Xu, Maj D.Mirmirani, and Petros A.Ioannou, "Adaptive sliding mode control design for a hypersonic flight vehicle," *Journal of Guidance, Control, and Dynamics*, vol. 27, no. 5, 2004, pp. 829-838.

[3] David O.Sigthorsson, et al, "Robust linear output feedback control of an airbreathing hypersonic vehicle," *Journal of Guidance, Control, and Dynamics*, vol. 31, no. 4, 2008, pp. 1052-1066.

[4] Michael A.Bolender and David B.Doman, "A non-linear model for the longitudinal dynamics of a hypersonic air-breathing vehicle," *AIAA Guidance, Navigation and Control Conference and Exhibit*, AIAA 2005-6255, 15-18 August 2005.

[5] Obaid Ur Rehman, Baris Fidan, and Ian R. Petersen, "Robust minimax optimal control of nonlinear uncertain systems using feedback linearization with application to hypersonic flight vehicles," *in Proc. 48th IEEE Conference on Decision and Control*, Shanghai, China, 2009, pp.720-726.

[6] Qian Wang and Robert F. Stengel, "Robust nonlinear control of a hypersonic aircraft," *Journal of Guidance, Control, and Dynamics*, vol. 23, no.4, July-August 2000, pp. 577-585.

[7] Qunya Yin, Jianqiang Yi, and Xiangmin Tan, "Time-varying sliding mode control for air-breathing hypersonic vehicles," *ICIC Express Letters - An International Journal of Research and Surveys*, vol. 5, no. 4(A), 2011, pp. 1031-1036.

[8] John D. Shaughnessy, S. Zane Pinckney, John D. McMinn, Christopher I. Cruz, and Marie-Louise Kelley, "Hypersonic vehicle simulation model: winged-cone configuration," *NASA Technical Memorandum 102610*, NASA Langley, 1991.

[9] Shahriar Keshmiri, Richard Colgren, and Maj Mirmirani, "Development of an aerodynamic database for a generic hypersonic air vehicle," *AIAA Guidance, Navigation and Control Conference and Exhibit*, AIAA 2005-6257, 15-18 August 2005.

[10] Abolfazl Jalilvand, Ali Kimiyaghalam, Ahmad Ashouri, and Meisam Mahdavi, "Advanced particle swarm optimization-based PID controller parameters tuning," *Proceedings of the 12th IEEE International Multitopic Conference*, December 23-24, 2008.

[11] Huanpao Huang, Hui Wan, and Jingqing Han, "Arranging the transient process is an effective method improved the robustness, adaptability and stability of closed-loop system," *Control Theory and Applications*, vol. 18, no. Suppl., August 2001, pp. 89-94.

[12] Baris Fidan, Maj Mirmirani, and Petros A. Ioannou, "Flight dynamics and control of air-breathing hypersonic vehicles: review and new directions", *AIAA International Space Planes and Hypersonic Systems and Technologies*, AIAA 2003-7081, 15-19 Decemeber 2003.

[13] Kevin P.Groves, Andrea Serrani, Stephen Yurkovich, Michael A.Bolender, and David B.Doman, "Anti-windup control for an air-breathing hypersonic vehicle model," *AIAA Guidance, Navigation and Control Conference and Exhibit*, AIAA 2006-6557, 21-24 August 2006.